

1 **WebPanel 1.** Description of the forecasted NEON lakes, overview of the FLARE configuration
2 for each lake, meteorological driver data, mean day-of-year null model, and guide to
3 reproducibility.

4 5 **NEON Lake temperature data**

6 We generated forecasts for the six NEON lakes in the conterminous USA (WebTable 1).
7 The six forecast sites were two paired lakes in the Great Lakes NEON ecoclimatic domain
8 (Crampton Lake, NEON site ID – CRAM; Little Rock Lake, NEON site ID - LIRO), two paired
9 lakes in the Northern Plains domain (Prairie Lake, NEON siteID – PRLA; Prairie Pothole,
10 NEON siteID - PRPO), and two paired lakes in the Southeastern domain (Barco Lake, NEON
11 siteID – BARC; Suggs Lake, NEON siteID - SUGG). We excluded the seventh NEON lake site
12 (Toolik Lake) since it was not part of a paired NEON set and it has major surface inflows, unlike
13 the other lakes.

14 Each lake had 5-10 water temperature sensors (Precision Measurement Engineering Inc.
15 T-Chain RS 232/485 thermistors) deployed at various depths in the water column. The first
16 sensor was deployed 0.05 m below the surface, with remaining depths dependent on the total
17 depth of the lake. Generally, sensors were deployed at more frequent intervals within the upper
18 1.05 m than at deeper depths. These discrete depth water temperature data are available from
19 NEON (NEON 2022a, b), and were accessed using the *neonstore* R package, which creates a
20 "store" of NEON data on a local computer and eases the iterative downloading of additional
21 NEON data without re-downloading data already within the store (Boettiger *et al.* 2021).

22 All data were filtered using the quality assurance codes provided by NEON. The 30-
23 minute data product was aggregated to the hour and only the 00:00-01:00 UTC hour was used
24 each day for assimilation and evaluation. The NEON (NEON 2022a, b) data were exported using
25 the *neon_export* function in the *neonstore* R package and archived at Thomas and Boettiger
26 (2022). Gaps in NEON's discrete depth water temperature dataset were filled using water
27 temperature data collected by a YSI EXO2 multiparameter sonde as part of NEON's water
28 quality data product (Hensley 2022).

29 30 **FLARE and GLM configuration**

31 Adapting FLARE to NEON lakes required configuring six unique GLM models with
32 each lake's bathymetry and physical specifications and developing functions to download and
33 process NEON water temperature data. Across all six lakes, we used the same initial default
34 GLM hydrodynamic parameters (Hipsey *et al.* 2019) and tuned the same set of three parameters
35 governing lake water temperature during data assimilation (*lw_factor*, *kw*, and *sed_mean_temp*).
36 Since none of the six NEON lakes have major surface inflows or outflows and prior applications
37 at a reservoir in Virginia showed limited sensitivity of forecast uncertainty to inflows (Thomas *et*
38 *al.* 2020), we parameterized each lake without inflows or outflows.

39 We parameterized the process uncertainty in water temperature to be the same across
40 sites and throughout the water column (standard deviation = 0.75°C). This value was based on
41 the findings of Thomas *et al.* (2020), in which FLARE's process uncertainty was estimated
42 across water column depths at a reservoir in Virginia. The process uncertainty was added to each
43 ensemble member and modeled depth at each daily timestep. Since we expect this uncertainty to
44 be correlated with depth (e.g., if the modeled temperature at a certain depth was 1°C warmer than
45 observed, nearby depths should also likely be too warm as well), we included a correlation
46 length that represents an exponential decay of correlations across depths (following Appendix A

47 in Lenartz *et al.* 2007). The decay in correlation results in stronger correlations in water
48 temperature at closer depths than further away depths. This decorrelation length parameter was
49 set to 2 m.

50 Similarly, observation uncertainty in water temperature data was set to be the same across
51 lakes and depths (standard deviation = 0.1°C), based on the FLARE application in Thomas *et al.*
52 (2020). Since observation uncertainty represents sensor and sampling uncertainty, we did not
53 expect observation uncertainty to be correlated with depth, and therefore the decorrelation length
54 for this uncertainty source was set to 0 m.

55 Parameter estimation using the ensemble Kalman filter (EnKF) uses the estimated
56 correlation between parameter values and the size of the errors between the predicted and
57 observed states across ensemble members (Evensen 2009). Ensemble members that require large
58 adjustments in the states to be consistent with observations will also adjust parameters that are
59 correlated with that error. One challenge with estimating parameters using the EnKF is that the
60 variation in parameter values across ensemble members collapses over time. The small variance
61 among ensemble members prevents the parameters from further adjusting to reduce new biases
62 in the model predictions (i.e., the calibration does not change through time).

63 As a result, parameter estimation methods using the EnKF need to use a technique to
64 prevent a collapse in variance. Here, we use a method called variance inflation, in which the
65 variance in parameter values among the ensemble members is increased at each time-step when
66 data assimilation occurs. The variance inflation increases the spread in the parameters among
67 ensemble members while maintaining the rank order of ensemble members. We used the same
68 variance inflation factor across all parameters and lakes (0.04).

69 The FLAREr R package that contains FLARE functions can be found in the Zenodo
70 repository (Thomas *et al.* 2022b), as well as the scripts for running FLARE at the six NEON
71 lakes (Thomas *et al.* 2022a). All analyses were conducted in R software version 4.1.1 (R Core
72 Team 2021).

73

74 **Meteorological inputs**

75 The forecasts were driven by numerical meteorological forecasts produced by NOAA's
76 Global Ensemble Forecasting System (GEFS) version 12 (Li *et al.* 2019). We automated the
77 downloading of ensemble members (n=31 total) from the NOAA GEFS output for each
78 0.5°×0.5° grid cell that included a NEON lake. NOAA GEFS generates weather forecasts at
79 multiple times per day (00:00, 06:00, 12:00, and 18:00 UTC), which vary in their forecast
80 horizon length (i.e., days into the future). We focused on the GEFS weather forecast that started
81 at 00:00 UTC each day, as 30 of its 31 ensemble members extended 35 days into the future on a
82 6-hour time step and included all meteorological variables required by the GLM as model driver
83 data. The 6-hour output resolution of each of the 30 ensemble members was temporally
84 disaggregated to 1-hour resolution for use in the GLM following Thomas *et al.* (2020).

85 We used a “stacked” GEFS product during the 1-month spin-up period. One challenge
86 when using data assimilation to set initial conditions and tune parameters is a potential mismatch
87 between the meteorological data used in the spin-up and data used for generating future
88 forecasts. Since observed and forecasted meteorology are rarely a 1:1 match, a smooth transition
89 from data assimilation to forecasting requires either the forecasted meteorology to be corrected
90 for the site or past meteorological forecasts to be used in place of observed meteorology for data
91 assimilation. Here, we used the latter option because NEON meteorological data has a 1.5-month
92 latency and often has gaps for some of the required meteorological variables. To develop a

93 “stacked” GEFS product, we also downloaded the 0-hour and 6-hour horizon of the forecasts that
94 were initiated every six hours at 06:00, 12:00, and 18:00 UTC each day (the 0-hour and 6-hour
95 for the 00:00 UTC forecast were already downloaded as part of the full 35-day horizon). We then
96 combined the temperature, relative humidity, and wind speed from the 0-hour horizon for all
97 NOAA GEFS forecasts. The flux variables (precipitation, longwave radiation, and shortwave
98 radiation) required using the 6-hour horizon because they integrate the 0th to 6th hour. The 0 and
99 6-hour horizons were used because they directly follow data assimilation in the GEFS, and
100 therefore are most closely aligned with observed meteorology. The resulting “stacked” product
101 was a 6-hr time-step meteorology product because the time step between the initiation of new
102 forecasts was six hours. The stacked data product was updated each time new GEFS forecasts are
103 available, and thus was near-real time.

104 To estimate the 10-day variance in air temperature that was used in the predictability
105 correlation analysis, we calculated the running standard deviation over a rolling 10-day window
106 between 18 May 2021 and 31 October 2021 from the “stacked” GEFS product. We used the
107 mean of the 10-day running standard deviation to represent air temperature variance for each
108 lake during the period that forecasts were generated.

109 All NOAA GEFS 1-hour forecasts and “stacked” products for the six NEON lakes are
110 archived at Thomas et al (2022b).

111

112 **Mean Day-of-Year Null Forecast**

113 We note that while the 1 to 3.5 years of data at the NEON lakes available for this day-of-
114 year (DOY) null model (see WebTable 1) is a shorter duration than the ~30 years of data
115 typically used in weather forecasting null climatology models, it still included all NEON data
116 available for each lake. Moreover, the DOY null model for the lake with just one year of data
117 (PRLA) performed similarly to the DOY null model for its paired lake (PRPO), which had three
118 years of data (Figure 2b).

119

120 **Guide to Reproducibility**

121 We have provided all code used to generate forecasts, analyze forecasts, and recreate
122 figures in this manuscript as a GitHub repository that has been archived on Zenodo (Thomas et
123 al. 2022a). There are three steps to the analysis that are documented as separate R scripts within
124 the repository. First, the “01_combined_paper_workflow.R” in the “workflows/neon_lakes_ms/”
125 directory of the repository obtains the NEON data and NOAA GEFS weather forecasts and then
126 runs FLARE on the six sites. Since this script runs 159 separate 35-day horizon forecasts for the
127 six lakes, the time required to generate all forecasts depends on the number and speed of
128 computer processors available and can be a multi-day execution. This first step produces a set of
129 output files for the GLM-based and day-of-year null forecasts in a “forecasts” directory.

130 Second, each ensemble forecast from the first step is aggregated to a mean with
131 predictive intervals and scored (by matching to the corresponding observation, if available), with
132 the summary statistics and observations saved as a set of scored files (one per output file) in a
133 “scores” directory in the repository. The scoring is generated by the “02_score_forecasts.R”
134 script located in the “workflows/neon_lakes_ms/” directory of the repository. While the scores
135 can be generated using output files from the first step, we also provide the output files as an
136 additional Zenodo repository (Thomas et al. 2022b) that can be downloaded and scored using the
137 script without needing to re-run the forecasts.

138 Third, the scored files are analyzed using an Rmarkdown script located in the main
139 directory of repository (“analysis_notebook.Rmd“) to produce the figures and data reported in
140 the text. The Rmarkdown script can use the scored files produced by the second step or the
141 scores files available in the additional Zenodo repository (Thomas et al. 2022b).

142 Our analysis can be reproduced by downloading the Zenodo GitHub repository and
143 running the three scripts associated with the steps described above. Re-running the full analysis
144 requires downloading R, Rstudio, and all the required packages, and as noted above, can take
145 multiple days of execution, depending on the computation available. We provide a script that
146 downloads the required packages (“install.R” in the main directory of the repository). However,
147 there is no guarantee that other versions of R and packages will produce the same results as
148 presented here.

149 To enable greater reproducibility, we adapted the GitHub repository (Thomas et al.
150 2022a) to generate a Binder that is produced by mybinder.org (Jupyter et al 2018). Mybinder.org
151 provides a web-based version of Rstudio for re-running our GitHub repository code that uses the
152 same version of R and R packages that we used in this analysis
153 (<https://mybinder.org/v2/zenodo/10.5281/zenodo.6267616/?urlpath=rstudio>). As a result, there is
154 more confidence that the analysis can be reproduced by harnessing the Binder infrastructure,
155 which directly re-runs the analysis on a remote server and provides an Rstudio interface via a
156 web browser for running the scripts described above for each of the three analysis steps.

157 There are important caveats to using the Binder. First, at the time of this analysis,
158 mybinder.org is free to use, and therefore its computational resources have limits and processing
159 times can be slow. Consequently, we do not recommend running the full generation of the 35-
160 day forecasts in the Binder. The Binder is ideally suited for exploring the scored forecasts and
161 reproducing the figures and values presented in the text (i.e., the “analysis_notebook.Rmd” script
162 described in the third step above). Second, at the time of this analysis, the Binder does not
163 always consistently launch when accessing the Binder link and occasionally the connection times
164 out. It may require accessing the Binder link again to get a successful launch of the R studio
165 interface.

166

167 **WebReferences**

- 168 Boettiger C, Thomas RQ, Laney C, and Lunch C. 2021. neonstore: NEON Data Store. R
169 package. CRAN repository. <https://cran.r-project.org/web/packages/neonstore/index.html>
170 Evensen G. 2009. Data Assimilation. Berlin, Heidelberg: Springer Berlin Heidelberg.
171 Hensley, R.T. 2022. NEON lakes Level 0 multisonde temperature data - 2021 ver 1.
172 Environmental Data Initiative repository.
173 <https://doi.org/10.6073/pasta/fbbd2d5f59a8d92c6865d57e7abae379> (Accessed 2022-01-
174 25).
175 Hipsey MR, Bruce LC, Boon C, *et al.* 2019. A General Lake Model (GLM 3.0) for linking with
176 high-frequency sensor data from the Global Lake Ecological Observatory Network
177 (GLEON). *Geosci Model Dev* **12**: 473–523.
178 Jupyter et al. 2018. Binder 2.0 - reproducible, interactive, sharable environments for science at
179 scale." Proceedings of the 17th Python in Science Conference (SCIPY 2018). Austin,
180 Texas: SciPy. <https://doi.org/10.25080/Majora-4af1f417-011>.
181 Lenartz F, Raick C, Soetaert K, and Grégoire M. 2007. Application of an Ensemble Kalman
182 filter to a 1-D coupled hydrodynamic-ecosystem model of the Ligurian Sea. *J Mar Syst*
183 **68**: 327–48.

184 Li W, Guan H, Zhu Y, *et al.* 2019. Prediction Skill of the MJO, NAO and PNA in the NCEP
185 FV3-GEFS 35-day Experiments. In: Science and Technology Infusion Climate Bulletin.
186 Durham, NC: NOAA's National Weather Service.

187 NEON. 2022a. Temperature at specific depth in surface water (DP1.20264.001). Dataset
188 available at <https://data.neonscience.org> (accessed 25 January 2022)

189 NEON. 2022b. Temperature at specific depth in surface water, RELEASE-2022
190 (DP1.20264.001). <https://doi.org/10.48443/g7bs-7j57>. Dataset available at
191 <https://data.neonscience.org> (accessed 25 January 2022)

192 R Core Team. 2021. R: A language and environment for statistical computing. Vienna, Austria:
193 R Foundation for Statistical Computing.

194 Thomas RQ and Boettiger C. 2022. RELEASE-2022 and provisional data for NEON
195 DP1.20264.001 at BARC, SUGG, CRAM, LIRO, PRLA, and PRPO. Zenodo repository.
196 <https://doi.org/10.5281/zenodo.5918679>

197 Thomas RQ, Figueiredo RJ, Daneshmand V, *et al.* 2020. A near-term iterative forecasting
198 system successfully predicts reservoir hydrodynamics and partitions uncertainty in real
199 time. *Water Resour Res* **56**: e2019WR026138.

200 Thomas RQ, McClure RP, Moore TM, Woelmer WM, Boettiger C, Figueiredo RJ, Hensley RT,
201 and Carey CC. 2022a. Near-term forecasts of NEON lakes reveal gradients of
202 environmental predictability across the U.S.: code (v1.1). Zenodo repository.
203 <https://doi.org/10.5281/zenodo.6674487>

204 Thomas RQ, McClure RP, Moore TM, *et al.* 2022b. Near-term forecasts of NEON lakes reveal
205 gradients of environmental predictability across the U.S.: data, forecasts, and scores.
206 Zenodo repository. <https://doi.org/10.5281/zenodo.6643596>

207 **WebTable 1.** Metadata of the six conterminous U.S. lake sites in the National Ecological Observatory Network. Variables that were
 208 included in the predictability correlation analysis included: latitude, maximum lake depth, fetch, volume, surface area, mean Secchi
 209 depth, mean annual temperature, mean annual precipitation, variance in air temperature, mean hydrological residence time, and
 210 catchment size.

siteID	Lake name	NEON Ecoclimatic domain	Latitude (°N)	Longitude (°E)	Elevation (m)	Maximum lake depth (m)	Fetch (m)	Volume (m ³)	Surface area (km ²)
BARC	Barco Lake	Southeast	29.675982	-82.008414	27	6	425	256888	0.12
SUGG	Suggs Lake	Southeast	29.68778	-82.017745	32	3	867	415356	0.31
CRAM	Crampton Lake	Great Lakes	46.209675	-89.473688	509	19	782	889734	0.26
LIRO	Little Rock Lake	Great Lakes	45.998269	-89.704767	501	10	623	466757	0.19
PRLA	Prairie Lake	Northern Plains	47.15909	-99.11388	565	4	1010	389429	0.23
PRPO	Prairie Pothole	Northern Plains	47.129839	-99.253147	579	4	511	158520	0.11

211
 212

213 **WebTable 1.** Continued

siteID	Mean Secchi depth (m)	Mixing regime	Mean annual temperature (°C)	Mean annual precipitation (mm)	Variance in air temperature (10-day standard deviation, °C)	Mean hydrological residence time (yrs)	Catchment size (km ²)	Number of years in time series for day-of-year null model
BARC	4.08	Polymictic	20.9	1308	1.09	3.3	0.8	2.4
SUGG	0.43	Polymictic	20.9	1308	1.09	1.6	36.9	3.4
CRAM	4.16	Dimictic	4.3	794	2.86	4.9	0.6	2.3
LIRO	4.37	Dimictic	4.4	796	2.86	3.4	0.9	3.1
PRLA	0.33	Polymictic	4.9	490	3.34	3.8	4.5	1.0
PRPO	0.40	Polymictic	4.9	494	3.39	3.2	1.4	2.0

214

215

216 **WebTable 1.** Continued

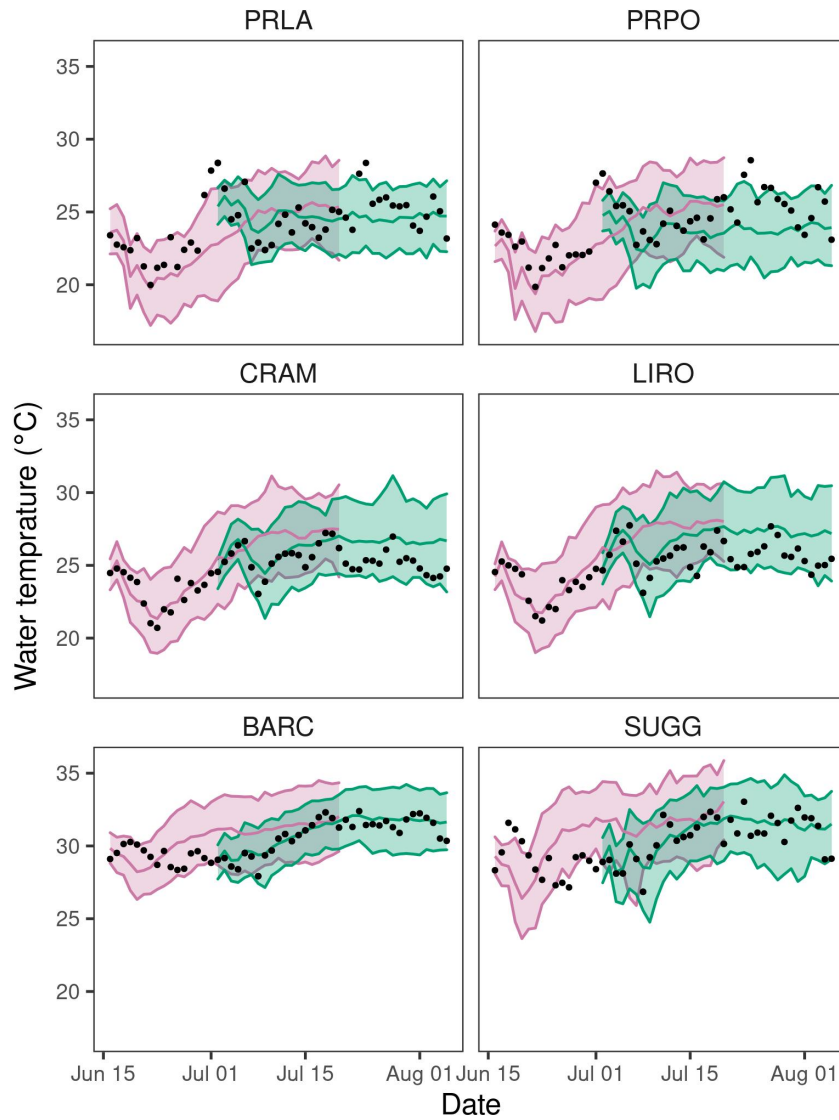
siteID	Catchment land cover	Depths with sensor observations (value is top of 0.25 m thick bin)	NEON Website
BARC	shrub/scrub	0.00, 0.25, 0.50, 0.75, 1.00, 1.25, 1.50, 2.00 2.50, 3.00	https://www.neonscience.org/field-sites/barc
SUGG	evergreen/forest; woody wetlands	0.00, 0.25, 0.50, 0.75, 1.00	https://www.neonscience.org/field-sites/sugg
CRAM	woody wetlands	0.00, 0.25, 0.50, 0.75, 1.00, 1.75, 2.00, 2.50, 3.25, 3.50, 4.25, 4.75, 5.00, 6.25, 6.50, 6.75, 7.75, 8.00, 8.50, 9.25, 9.50, 10.25, 10.75, 11.00 12.00, 12.50, 13.50, 14.00, 15.50	https://www.neonscience.org/field-sites/cram
LIRO	deciduous forest; mixed forest	0.00, 0.25, 0.50, 0.75, 1.00, 1.25, 1.50, 2.00, 2.25, 2.50, 2.75, 3.00, 3.25, 3.50, 4.00, 4.25, 4.50, 4.75, 5.00, 5.75, 6.00, 6.75	https://www.neonscience.org/field-sites/liro
PRLA	grassland/herbaceous	0.00, 0.25, 0.50, 0.75, 1.00, 1.25, 1.50, 1.75, 2.00	https://www.neonscience.org/field-sites/prla
PRPO	grassland/herbaceous	0.00, 0.25, 0.50, 0.75, 1.00	https://www.neonscience.org/field-sites/prpo

217

218 **WebTable 2.** Forecast accuracy, defined as root-mean square error (RMSE) at 1-day ahead, and
 219 forecast accuracy degradation, defined as the difference in maximum and minimum RMSE
 220 across the 35-day forecast horizon. We used Spearman rank correlations to quantify the
 221 relationships between morphometric, hydrological, ecological, and meteorological characteristics
 222 and mean forecast accuracy and accuracy degradation for each lake. To ease interpretation of the
 223 correlation coefficient, we negated RMSE so positive correlations are associated with higher
 224 accuracy. Given the extremely limited sample size of lakes (n=6), which is too small for reliable
 225 p-values for rho, we focused our interpretation on Spearman rho correlations $|\geq| 0.5$ (included
 226 here).

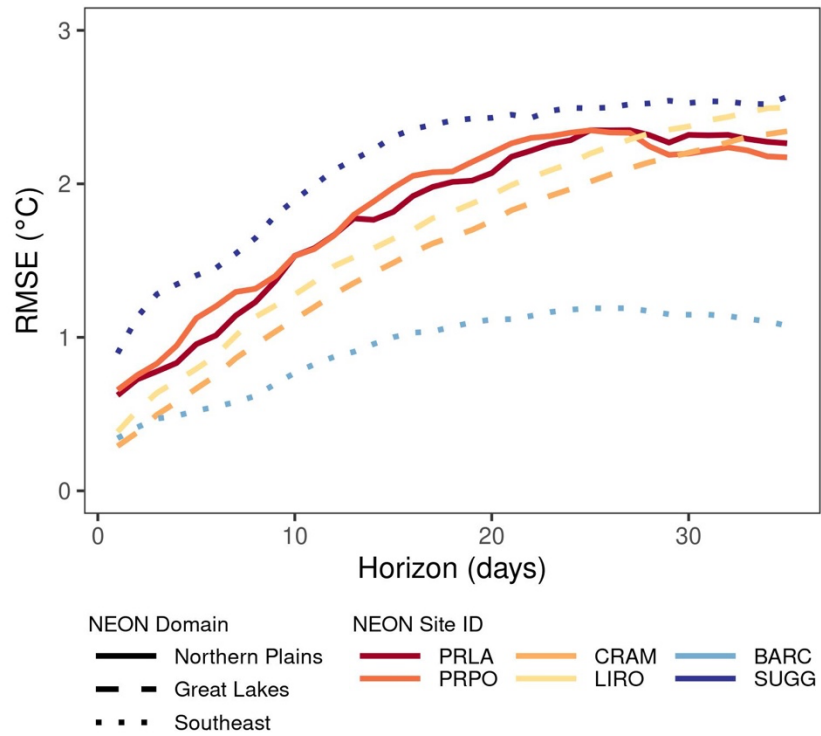
variable	metric	rho
Catchment size	accuracy	-0.94
Fetch	accuracy	-0.71
Maximum depth	accuracy	0.81
Water clarity (Secchi depth)	accuracy	0.60
Mean annual air temperature	degradation	-0.79
Water clarity (Secchi depth)	degradation	0.60
Volume	degradation	0.60

227
 228



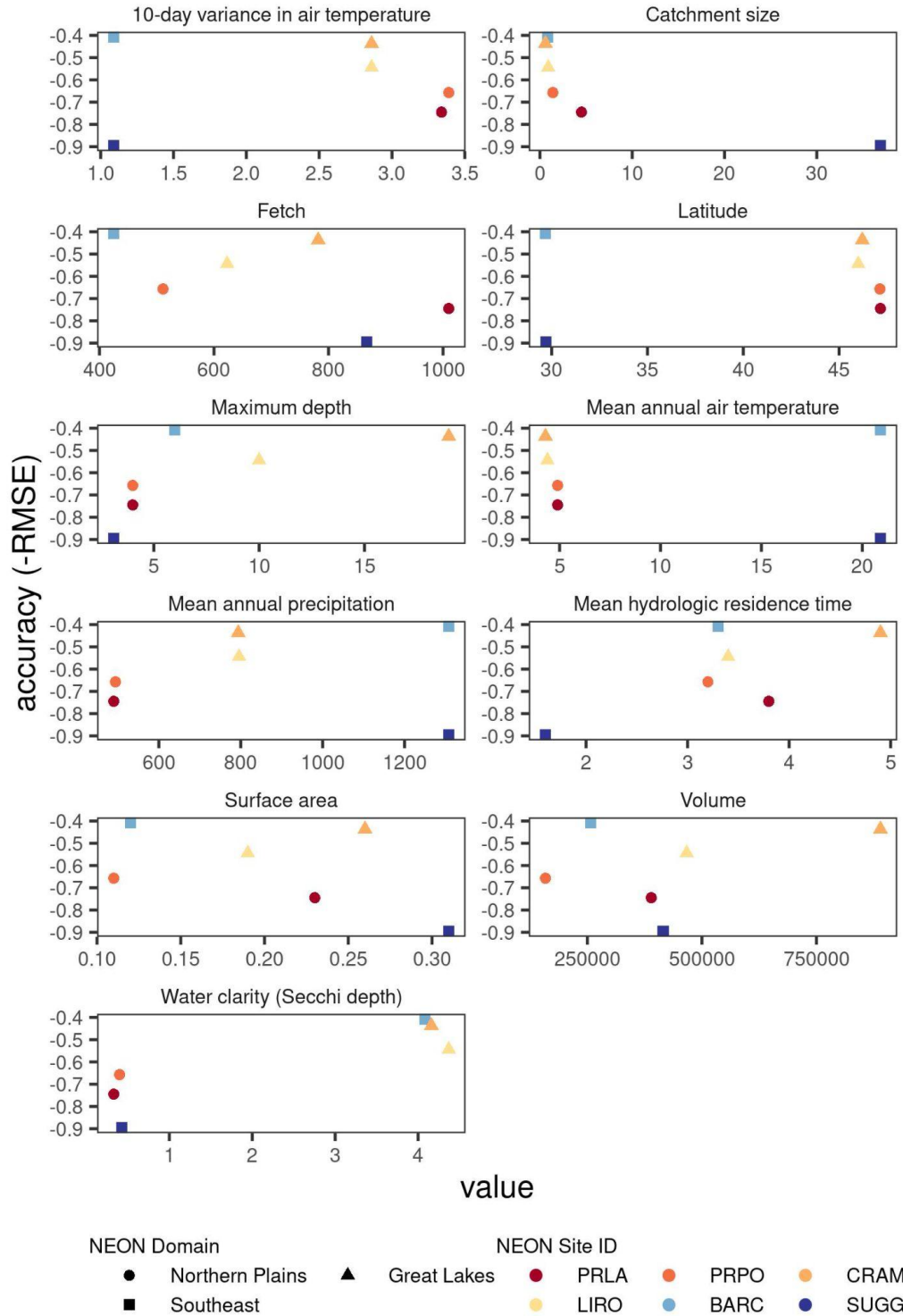
Forecast start date 2021-06-15 2021-07-01

229
 230 **WebFigure 1.** Example 35-day forecasts of surface water temperature that were initiated on
 231 2021-06-15 and 2021-07-01. The shaded region represents the 10% and 90% quantiles. The
 232 observations (black dots) are provided for reference.
 233



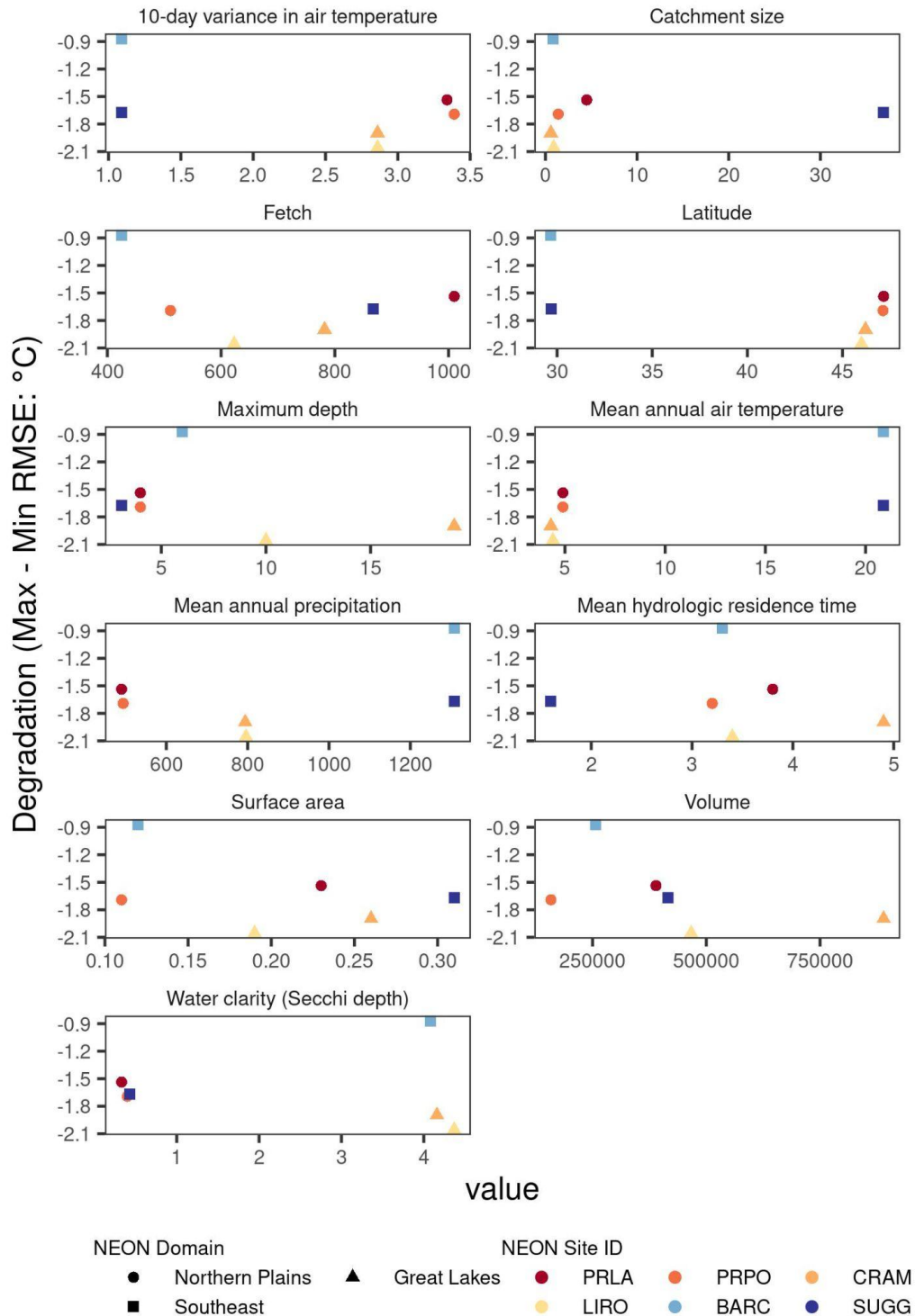
235
 236
 237
 238
 239
 240

WebFigure 2. Forecast accuracy for water temperature at all depths in each lake aggregated together. Accuracy is defined by RMSE (root-mean square error in °C), calculated separately for each 1 to 35-days ahead (horizon) at the six NEON lakes.



241
 242
 243
 244
 245
 246
 247

WebFigure 3. Relationships between forecast accuracy (y-axis) and the morphometric, hydrological, ecological, and weather characteristics included in Figure 3 (x-axis). We negated RMSE (root-mean square error in °C), so positive correlations are associated with higher accuracy. WebTable 1 includes the units for each variable.



248
249

250 **WebFigure 4.** Relationships between forecast accuracy degradation (y-axis) and the
 251 morphometric, hydrological, ecological, and weather characteristics included in Figure 3 (x-
 252 axis). Degradation is defined as the difference in RMSE (root-mean square error in °C)
 253 between the maximum and minimum RMSE over the 35-day forecast horizon. WebTable 1 includes the
 254 units for each variable.